THE ASTROPHYSICAL JOURNAL, 547:109–116, 2001 January 20

MORPHOLOGY-DENSITY RELATION FOR SIMULATED CLUSTERS OF GALAXIES IN COLD DARK MATTER–DOMINATED UNIVERSES

TAKASHI OKAMOTO
Division of Physics, Graduate School of Science, Hokkaido University, Sapporo 060-0810, Japan; okamoto@astro1.sci.hokudai.ac.jp
AND
MASAHIRO NAGASHIMA
National Astronomical Observatory, Mitaka, Tokyo 181-8588, Japan; masa@th.nao.ac.jp
Received 2000 September 14; accepted 2000 September 15

ABSTRACT

We present a model to investigate the formation and evolution of cluster galaxies using cosmological high-resolution N-body simulations. The N-body simulations are used to construct merging history trees of dark halos. Gas cooling, star formation, supernova feedback, and mergers of galaxies within dark halos are included by using simple prescriptions taken from semianalytic models of galaxy formation. In this paper, we examine the merger-driven bulge formation model and represent the morphology-density relation of cluster galaxies at $z = 0$. We find that this morphological evolution model can explain the distribution of elliptical galaxies in the clusters well and cannot reproduce the distribution of S0 galaxies. This result suggests that the elliptical galaxies are mainly formed by the major mergers, while, in the S0 formation, processes other than major mergers play an important role.

Subject headings: galaxies: clusters: general — galaxies: halos — galaxies: interactions

1. INTRODUCTION

It is well established that galaxy populations vary with the density of neighboring galaxies in clusters of galaxies (Dressler 1980). This morphology-density relation (hereafter MDR) indicates that dynamical processes that depend on environment of each galaxy mainly affect the final configuration of the stellar component. This impression seems to be supported by the *Hubble Space Telescope* images of clusters at intermediate redshifts, which show an abnormally high proportion of spiral and irregular types at $z \sim 0.5$ and an increase of the S0 fraction toward the present time (Couch et al. 1994; Dressler et al. 1997).

Some mechanisms that may transform one morphological type into another have been proposed, for example, ram-pressure stripping of interstellar medium of spirals by a intracluster medium (Gunn & Gott 1972; Fujita & Nagashima 1999), galaxy harassment by cumulative tidal interactions in clusters (Moore et al. 1996; Moore, Lake, & Katz 1998), and galaxy mergers (Toomre 1977). N-body simulations have confirmed that merging disk galaxies produce galaxies resembling ellipticals as merger remnants (e.g., Barnes 1996), so that the galaxy merger is a favorite explanation for the predominance of ellipticals and S0s in rich clusters (Kauffmann, White, & Guiderdoni 1993; Kauffmann 1996; Baugh, Cole, & Frenk 1996).

The purpose of our study is to check this *major merger hypotheses* by investigating the MDR for the simulated clusters in the cosmological context. For this purpose, it is difficult in the present situation to use numerical simulations including both gravity and gas dynamics (e.g., Katz, Hernquist, & Weinberg 1992; Evrard, Summers, & Davis 1994), because such simulations are expensive in CPU time and so only a limited range of parameter space can be explored with an insufficient spatial resolution.

Semianalytic modeling of galaxy formation has already proved to be a powerful technique (e.g., Kauffmann et al. 1993; Cole et al. 1994). However, we cannot identify the position of galaxies by such approaches, because these models follow the collapse and merging histories of dark halos by using a probabilistic method on the mass distribution based upon an extension of the Press-Schechter formalism (Press & Schechter 1974; Bond et al. 1991; Bower 1991; Lacey & Cole 1993).

One approach to identify the position and velocity of each galaxy is to track the merging histories of dark halos by using N-body simulations and to combine them with the simple prescriptions of the semianalytic models (Roukema et al. 1997; Kauffmann et al. 1999; Benson et al. 2000). These schemes, however, do not deal with the substructures within dark halos. Since the dynamics within clusters may strongly affect the evolution of cluster galaxies (Okamoto & Habe 1999, 2000), we should use a new galaxy tracing method.

In this paper, we adopt the galaxy tracing method provided by Okamoto & Habe (1999, 2000), which enables us to trace the individual galactic dark halos within dense environments using high-resolution N-body simulations; that is, we can obtain the three-dimensional distribution of the galaxies within clusters. Our formula of modeling gas cooling, star formation, supernova feedback, and galaxy mergers is directly taken from the previous semianalytic work. We also adopt a merger-driven scheme for the production of galactic bulges and the way of the morphological classification based on bulge-to-disk ratios as earlier studies (Kauffmann et al. 1993; Baugh et al. 1996).

In § 2 we describe a brief outline of the galaxy formation model used here. We show the results about the morphology of the galaxies in § 3. These results are discussed in § 4.

2. MODEL

We examine the evolution of cluster galaxies in the standard cold dark matter (SCDM) universe ($\Omega_0 = 1$, $h \equiv H_0/100$ km s^{-1} Mpc^{-1} $= 0.5$, $\sigma_8 = 0.67$) and the open CDM (OCDM) universe ($\Omega_0 = 0.3$, $h = 0.7$, $\sigma_8 = 1.0$). The baryon density is set to $\Omega_b = 0.1$ and 0.03 for SCDM and OCDM, respectively.

The outline of the procedures of galaxy formation is as follows. At first, the merging path of galactic halos are realized by the cosmological high-resolution N-body simulations. Next, in each merging path, evolution of the baryonic component, namely, gas cooling, star formation, and supernova feedback, are calculated based on Kauffmann et al. (1993) and Cole et al. (1994). We refer a system consisting of the stars and cooled gas as a *galaxy*. When two or more dark halos merge together, we estimate the merging timescale based on the dynamical friction timescale. When the merging of galaxies occurs, we change the morphology of the merger remnant by the type of the merger. Finally, we calculate the luminosity and color of each galaxy. Through the above procedures, we obtain the morphological distribution of cluster galaxies.

2.1. *N-Body Calculation and Merging of Dark Halos*

The merging histories of galactic dark halos are realized using the same method and simulation data as Okamoto & Habe (2000). Note that they trace *halo-stripped galaxies* as well as the galactic halos because halo disruption is probably due to lack of dissipative processes, which are not included in the N-body simulations (Summers, Davis, & Evrard 1995). While the merging histories are constructed with a 0.5 Gyr time step in their paper, here we adopt half of the time step for high redshifts ($z \gtrsim 2.0$) at which the galactic halos form and merge violently (Okamoto & Habe 2000). This improvement, however, hardly changes our results.

2.2. *Model of Galaxy Formation*

The following prescriptions are almost the same as the previous ordinary semianalytic models.

For simplicity, a dark halo is modeled as an isothermal sphere whose mass and radius are taken from N-body data. The source of the diffuse gas in a halo is hot gas contained in its progenitor halos and in the accreting matter. The baryon fraction of the accreting matter is defined as $f_b = \Omega_b/\Omega_0$. We assume that the hot gas has the distribution that parallels to that of the dark matter with the virial temperature of the halo. When a galactic halo is tidally stripped, the hot gas in the halo is also stripped proportional to the amount of the stripped dark matter.

The cooling timescale, $\tau_{\rm cool}$, is obtained as a function of the radius from the hot gas density profile, the temperature of the gas, and the cooling function $\Lambda(T)$ as follows,

$$\tau_{\rm cool} = \frac{3}{2}\frac{\rho(r)}{\mu m_{\rm p}}\frac{kT}{n_{\rm e}^2\Lambda(T)}, \quad (1)$$

where μm_p is the mean molecular weight, $n_e(r)$ is the electron number density at the radius r, and k is the Boltzmann constant. Using the zero-metallicity and solar-metallicity cooling functions given by Sutherland & Dopita (1991), the cooling efficiency depending on the metallicity of the gas are calculated by interpolation and extrapolation.

When a halo mass becomes more than double of the mass at the forming time, the diffuse hot gas contained in the halo is reheated by shock to the virial temperature of the halo (Somerville & Primack 1999). We refer this epoch as the reheating time of the halo. The cooling radius, $r_{\rm cool}$, is defined as a radius at which the cooling timescale, $\tau_{\rm cool}$, equals to the elapsed time from the last reheating time of the halo, t. The hot gas that distributes between $r_{\rm cool}(t)$ and $r_{\rm cool}(t + \Delta t)$ is cooled and added to the cold gas reservoir of the galaxy during the time-step, Δt.

The star formation in disks is described by the following simple law:

$$\dot{M}_* = \frac{M_{\rm cold}}{\tau_*}, \quad (2)$$

$$\tau_* = \tau_*^0\left(\frac{\tau_{\rm dyn}}{\tau_{\rm dyn}^0}\right), \quad (3)$$

where equation (2) denotes the rate of stars newly formed, τ_*^0 is the star formation timescale of the galaxies that form at $z = 0$, $\tau_{\rm dyn} \equiv r_{\rm halo}/V_c$ is the dynamical timescale of the galaxies, and $\tau_{\rm dyn}^0$ indicates the dynamical timescale of a halo that forms at $z = 0$. Here we assume that the star formation timescale is proportional to the dynamical timescale. We calculate $\tau_{\rm dyn}^0$ according to the virial theorem and the spherical collapse model. The star formation timescale at $z = 0$, τ_*^0, is a free parameter and we set to 5 Gyr in this paper. We have confirmed that this parameter does not affect strongly on the morphology of the cluster galaxies.

The feedback process by supernovae of massive stars has many uncertainties actually, therefore we adopt a simple description (Cole et al. 1994),

$$\Delta M_{\rm reheat} = \left(\frac{V_c}{V_{\rm hot}}\right)^{-\alpha_{\rm hot}}\dot{M}_*\,\Delta t \equiv \beta\dot{M}_*\,\Delta t, \quad (4)$$

where $V_{\rm hot}$ and $\alpha_{\rm hot}$ are free parameters. When adopting $\alpha_{\rm hot} = 2$, equation (4) corresponds to the formula in Kauffmann et al. (1993), and Cole et al. (1994) used $\alpha_{\rm hot} = 5.5$ in their fiducial model.

When two or more halos merge together, we identify a galaxy contained in the largest progenitor as the central galaxy of the new common halo. Other galaxies are identified as satellites. These satellites merge with the central galaxy when the elapsed time from the last reheating time exceeds the dynamical friction timescale (Binney & Tremaine 1987),

$$\tau_{\rm mrg} = \frac{1.17 r_{\rm halo}^2 V_c}{\ln\Lambda G M_{\rm sat}}, \quad (5)$$

where $r_{\rm halo}$ and V_c are the radius and circular velocity of the new common halo, respectively, $M_{\rm sat}$ is the total mass of a halo to which the satellite belonged as a central galaxy or the mass of stars and cold gas in the case that the satellite was a halo-stripped galaxy, and $\ln\Lambda$ is the Coulomb logarithm, which is approximated as $\simeq \ln(1 + M_{\rm halo}^2/M_{\rm sat}^2)$ (Somerville & Primack 1999). When the mass growth of the common halo satisfies the reheating condition, the elapsed time from the last reheating time is recalculated because orbits of satellites may be violently disturbed in such a case.

When a satellite galaxy merges with a central galaxy and the mass ratio of the galaxy with smaller mass to that with larger mass,

$$R = \frac{(M_{\rm stars} + M_{\rm cold})_{\rm acc.sat.}}{(M_{\rm stars} + M_{\rm cold})_{\rm cen.gal.}}, \quad (6)$$

TABLE 1

FEEDBACK PARAMETERS FOR MODELS

Model	V_{hot} (km s^{-1})	α_{hot}
A......	280	2
B......	140	2
C......	200	5.5

is larger than f_{bulge}, all stars of the satellite and disk stars of the central galaxy are incorporated with the bulge of the central galaxy. Then cold gases of both galaxies turn to stars in the bulge by *starburst*.

If the mass ratio, R, does not exceed the value of the parameter f_{bulge}, the merger is classified as minor. In the minor merger, the disk of the central galaxy is preserved and no starburst takes place. In our model, half of the stars from satellites are added to the bulge of the central galaxy, and the rest are added to the disk of the central galaxy according to the results of simulations by Walker, Mihos, & Hernquist (1995). In their simulations, a satellite with total mass equal to 10% of the central disk galaxy mass merges with it, and then, roughly 50% of the satellite's stars sink to the core of the central galaxy, while the rest are ripped off and added to the disk of the central galaxy. There are two different ways to deal with the minor mergers in semianalytic models. In one scheme, all stars from satellites are added to the disk of the central galaxy (e.g., Kauffmann et. al. 1993), and in the other scheme, they are added to the bulge of the central galaxy (e.g., Baugh et. al. 1996). We find that there is little difference between our results using these three prescriptions.

We adopt $f_{bulge} = 0.3$ for SCDM according to the numerical simulations (Barnes 1996). Since early formation of the cluster prevent galaxy mergers in OCDM, we use $f_{bulge} = 0.2$ for OCDM in order to reproduce the observed E + S0 fraction roughly (see § 3).

Chemical evolution is treated in almost the same way as described in Kauffmann & Charlot (1998). The instantaneous recycling approximation is adopted. The amount of metals ejected from supernovae is characterized by y, which is heavy element yield for each generation of stars. The fraction f of the ejecta is ejected directly into the hot gas, and the rest is incorporated with the cold gas. We adopt $y = 2\ Z_\odot$ and $f = 0.3$, which are the same values as the strong feedback model in Kauffmann & Charlot (1999). The gas fraction returned by evolved stars, R, is 0.25 in this paper. Simultaneously, the supernovae heat up the surrounding cold gas, then metals contained in the cold gas are also returned to the hot gas. The chemical evolution mainly affects on the colors of the galaxies. Therefore, the value of the yield is not important in this paper. The colors of the cluster galaxies will be discussed in our next paper.

In order to compare our results with observations directly, stellar population synthesis model must be considered. We use the model by Kodama & Arimoto (1997) with the Salpeter's (1955) initial mass function having a slope of 1.35 and mass range between 0.1 $M_\odot$ and 60 $M_\odot$. The range of stellar metallicity Z_* of simple stellar populations is 0.0001 $\sim$ 0.05. The luminosity of disks and bulges is given by this model in each band according to the metalicities and ages of stars.

2.3. *Identification of Morphology*

Morphology of each galaxy is determined by the B-band bulge-to-disk luminosity ratio (B/D). In this paper, galaxies with $B/D \geq 1.52$ are identified as ellipticals, $0.68 \leq B/D < 1.52$ as S0s, and $B/D < 0.68$ as spirals, according to the results of Simien & de Vaucouleurs (1986). Although it has

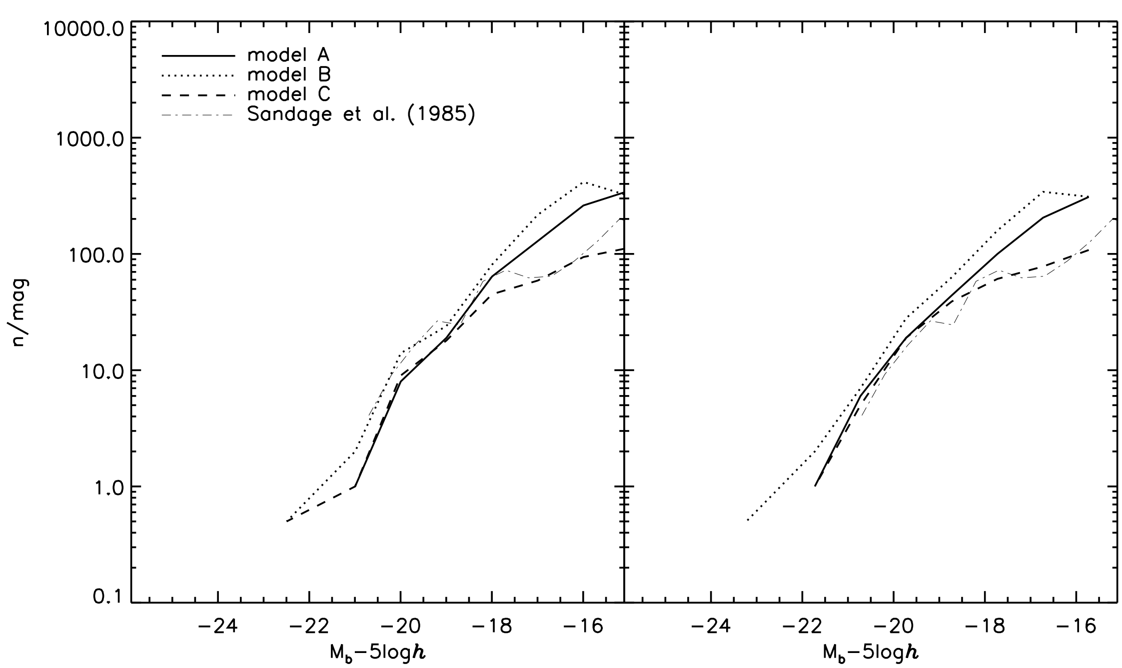

FIG. 1.—Luminosity functions of cluster galaxies. The left and right panels show those in SCDM and OCDM, respectively, and the thick solid, dotted, and dashed lines indicate those of the model A, B, and C, respectively. The thin dot-dashed line is the luminosity function of the Virgo cluster galaxies by Sandage et al. (1985).

been shown that this method for classification reproduces observations well by Kauffmann et al. (1993) and Baugh et al. (1996), it should be noted that our scheme for determining morphologies is not the same perfectly as the Dressler's (1980) to which we compare our results in this paper. We will discuss the systematics for the different definitions of morphologies in § 4.

2.4. *Parameter Sets*

The feedback is a key process that determines the features of galaxies (e.g., Kauffmann & Charlot 1998). Therefore, we use three type of feedback models in this paper (Table 1). The model A is a strong feedback model and B is a normal feedback model. In these two models $\alpha_{\rm hot}$ is set to 2. In the model C, we adopt $\alpha_{\rm hot} = 5.5$, which is used in the fiducial model of Cole et al. (1994), while $V_{\rm hot}$ is equal to 200 km s^{-1} that is large compared to theirs.

In Figure 1 we show the *B*-band luminosity functions of model galaxies. The thick solid, dotted, and dashed lines indicate the luminosity functions given by models A, B, and C, respectively, and the thin dot-dashed line indicates the observed luminosity function of the Virgo cluster (Sandage, Binggeli, & Tammann 1985). The model C reproduces the observed luminosity function well by flattening the faint-end slope of the luminosity function. This is caused by strong feedback to galaxies with low circular velocities compared to the model A and B due to $\alpha_{\rm hot} = 5.5$.

3. MORPHOLOGY OF THE CLUSTER GALAXIES

3.1. *Morphological Fraction*

In Figure 2, the E+S0 fractions of our cluster galaxies are shown as a function of absolute *B*-band magnitude. The observed curve for the Virgo cluster galaxies is taken from Sandage et al. (1985). All our models show the observational trend. It is, thus, found that the merger-induced bulge formation naturally increases the fraction of bulge-dominated galaxies toward a bright end. In the model C, the clusters do not have early-type galaxies sufficiently. This is probably caused by the lack of S0 galaxies as we show below.

3.2. *Morphology-Density Relation*

The MDRs for the simulated clusters are represented in Figure 3 using the same luminosity cutoff and definition of the local projected density as Dressler (1980), i.e., the local projected density is defined by nearest 10 neighbors having the luminosity $M_V - 5 \log h < -18.9$. The projected density is calculated in *x*-*y*, *y*-*z*, and *z*-*x* projections for each model. The morphological fractions of our models and Dressler's (1980) are represented by thick and thin lines, respectively. We attach the 1 σ error bars to the elliptical fractions according to the number of the galaxies in each density bin.

In all models, the E fractions increase toward the high-density regions, and this is consistent with the observed trend. The S0 fractions, however, are much smaller than the observed fraction and do not represent the observed trend of the moderate increase toward the high-density regions. We then examine whether such deficiency of S0 galaxies within the simulated clusters can be solved by adjusting the $f_{\rm bulge}$ and the B/D classification in the next subsection.

3.3. *Dependence on Model Parameters*

Since there is considerable scatter in the relationship between the bulge-to-disk ratio and Hubble T-type (Baugh

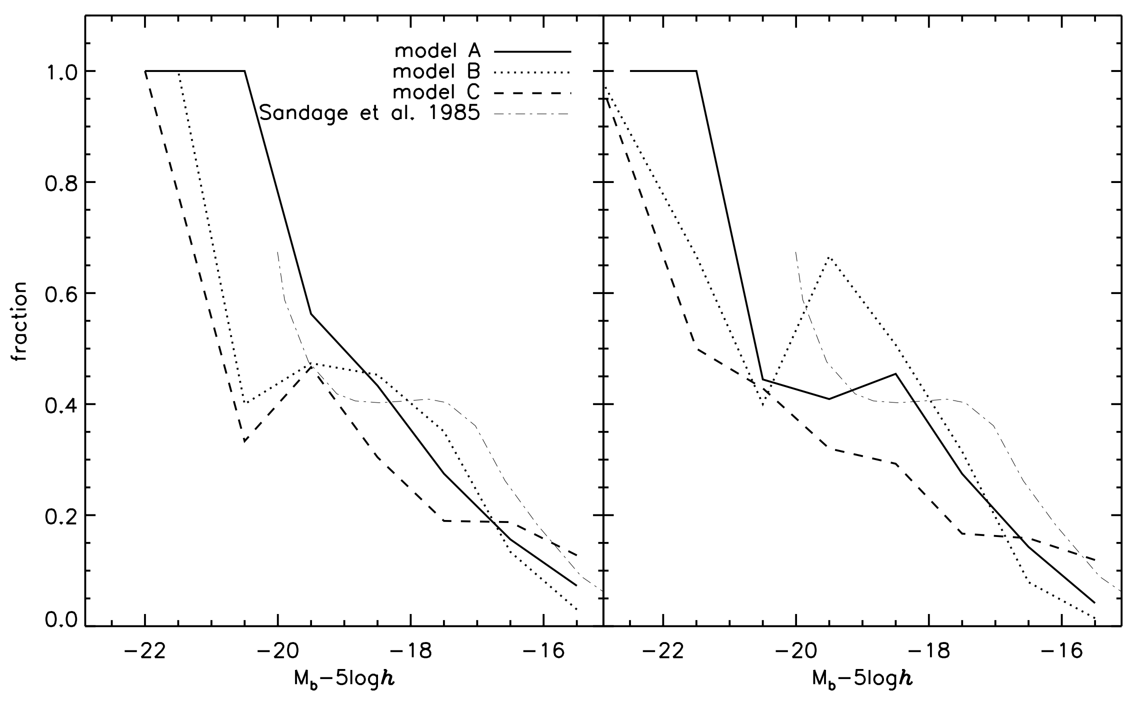

FIG. 2.—E+S0 fractions of cluster galaxies as a function of absolute *B* magnitude for SCDM (*left panel*) and OCDM (*right panel*). The thick solid, dotted, and dashed lines indicate the model A, B, and C, respectively. The thin dash-dotted line shows the observational result for the Virgo cluster taken from Sandage et al. (1985).

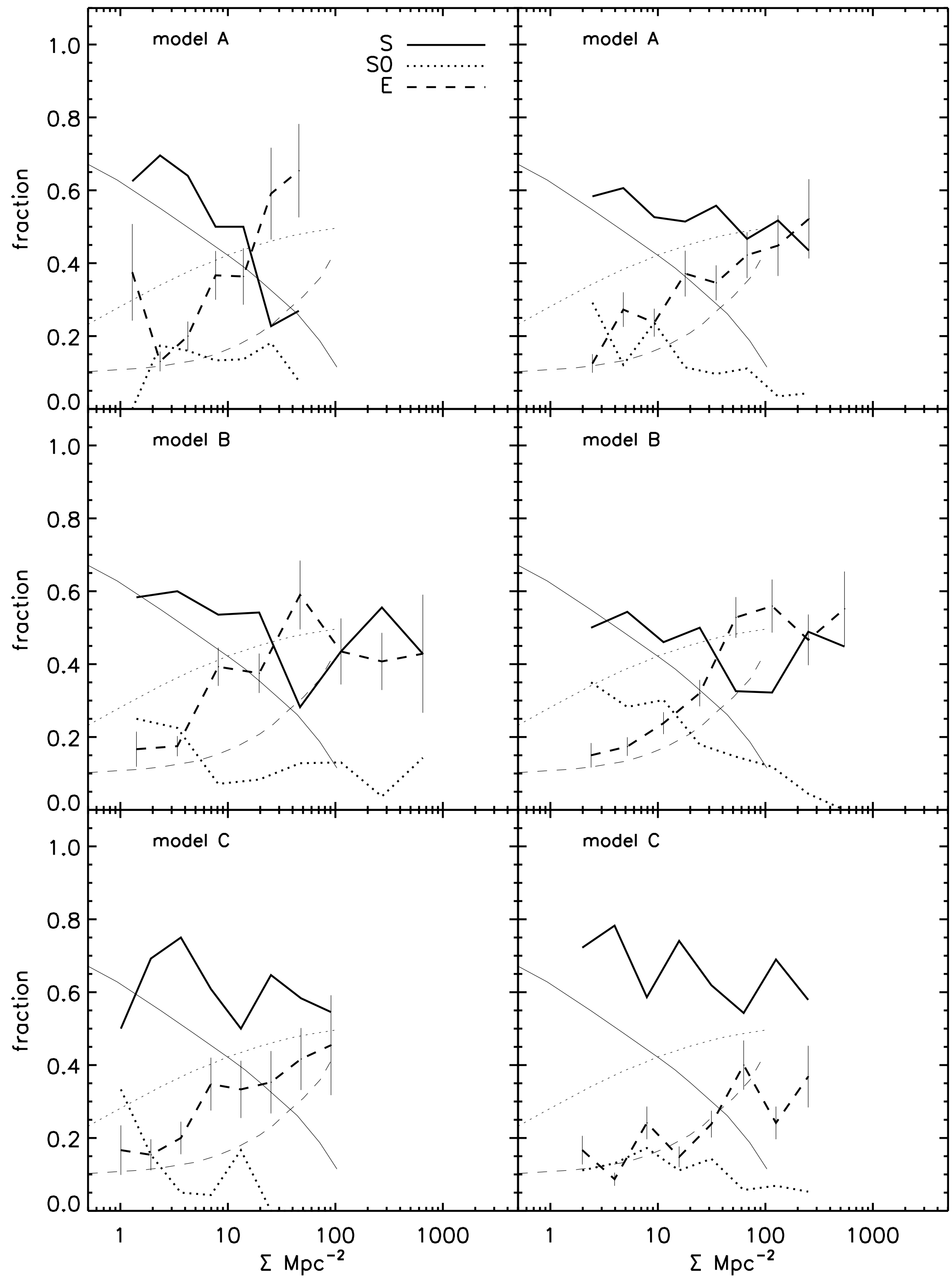

FIG. 3.—Morphology-density relations for cluster galaxies. The left and right panels show the results for SCDM and OCDM, respectively. The thick lines are the morphological fraction of model galaxies, and the thin lines are those of the observed cluster galaxies by Dressler (1980). S, E, and S0 fractions are represented by the solid, dotted, and dashed lines, respectively. We show the error bars for the elliptical fractions, which are 1σ Poissonian uncertainties estimated from the number of galaxies in each bin.

et al. 1996), we should examine the case in which we adopt different values of B/D for the classification of the galaxies. We also investigate how the parameter, $f_{\rm bulge}$, affects on the MDRs.

To study the influence of the choice of these parameters, we use the model C in OCDM. By this model, the luminosity function and the distribution of the elliptical galaxies are in good agreement with the observations, the E+S0 fraction, however, is insufficient. The B/D range for S0s and the value of the $f_{\rm bulge}$ in new models are listed in Table 2.

First, we adapt the new B/D classification, that is, galaxies with $B/D \geq 1.52$ are identified as ellipticals, $0.25 \leq B/$

TABLE 2

S0 DEFINITION AND VALUES OF f_{bulge}

Model	S0 B/D Definition	f_{bulge}
C_1......	0.25–1.52	0.2
C_2......	0.68–1.52 (standard)	0.1
C_3......	0.25–1.52	0.1
C_4......	0.68–4.00	0.1

$D < 1.52$ as S0s, and $B/D < 0.25$ as spirals. We call this model the model C_1. In this definition, spirals with high B/D in the standard definition are identified as S0s. In Figure 4 we plot the E+S0 fraction of this model (*solid line*). The fraction is slightly increased, however, still below the observation. The MDR of this model is presented in Figure 5. Although the S0 fraction is increased by adopting wider B/D range for S0s, the fraction is too small, especially in the high-density regions. Koopmann & Kenney (1998) indicated that galaxies with low central concentration (i.e., low B/D), with which they should be classified into spiral galaxies such as Sa galaxies in field environment, were often identified as S0 galaxies owing to their low star formation rates. They suggested that misleading classification of the low central-concentration galaxies as S0s might account for a part of domination of S0 galaxies in cluster environment. Our result, however, shows that the distribution of the S0s is not reproduced by the major merger-driven bulge formation even when we identify the galaxies with low B/D as S0s.

Next, we set f_{bulge} to 0.1 in order to increase the E+S0 fraction. We call this model the model C_2. The E+S0 fraction of model C_2 with the B/D classification in § 2.3 is shown in Figure 4. The fraction is fairly increased than the model C and show better agreement with the observation. In the top panel of the Figure 6, we show the MDR of this model. It is found that both of E and S0 fraction are increased, the shortage of S0s is, however, still significant. We then examine the case in which we adopt the same B/D classification as the model C_1 for the galaxies in the model C_2 in order to increase the S0 fraction. This model is referred as the model C_3. In this case, too many spirals are moved to S0s in the low-density regions, and the morphological fractions in the high-density regions are hardly changed (the middle panel of Fig. 6). It is also interesting to investigate how the MDR changes by changing the threshold value of the B/D between E and S0. We identify the galaxies with $B/D \geq 4$ as Es, and then the galaxies with $0.68 \leq B/D < 4$ as S0s (model C_4). The MDR in this case is indicated in the bottom panel of Figure 6. While the S0 fraction becomes comparable with the observation in the low-density regions,

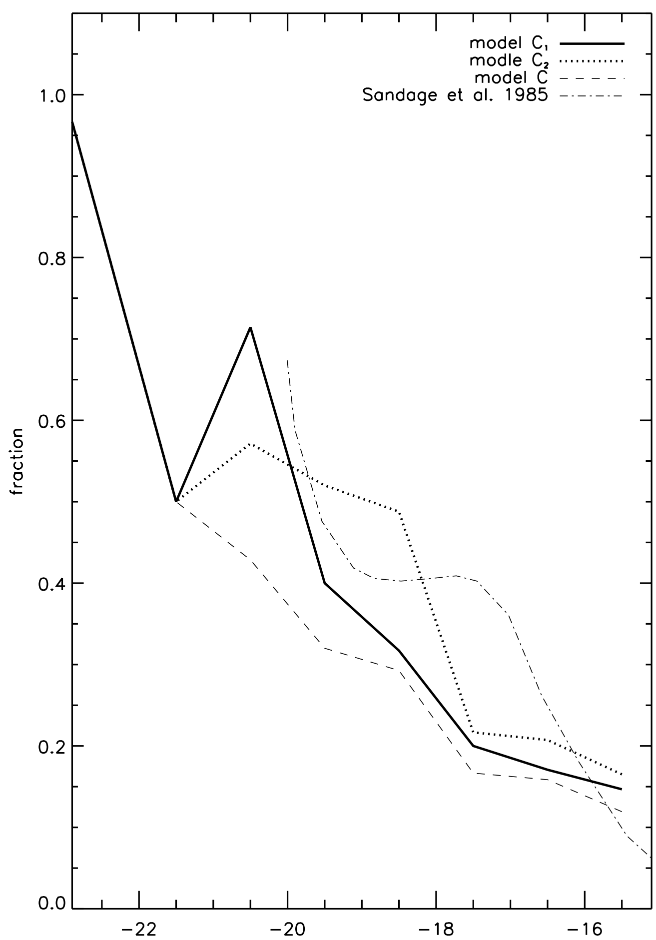

FIG. 4.—Same as Fig. 2, but for the model C_1 (*thick solid line*) and C_2 (*thick dotted line*). For comparison, the fraction in model C and the fraction of the Virgo clusters are represented by the thin dashed line and the thin dash-dotted lines, respectively.

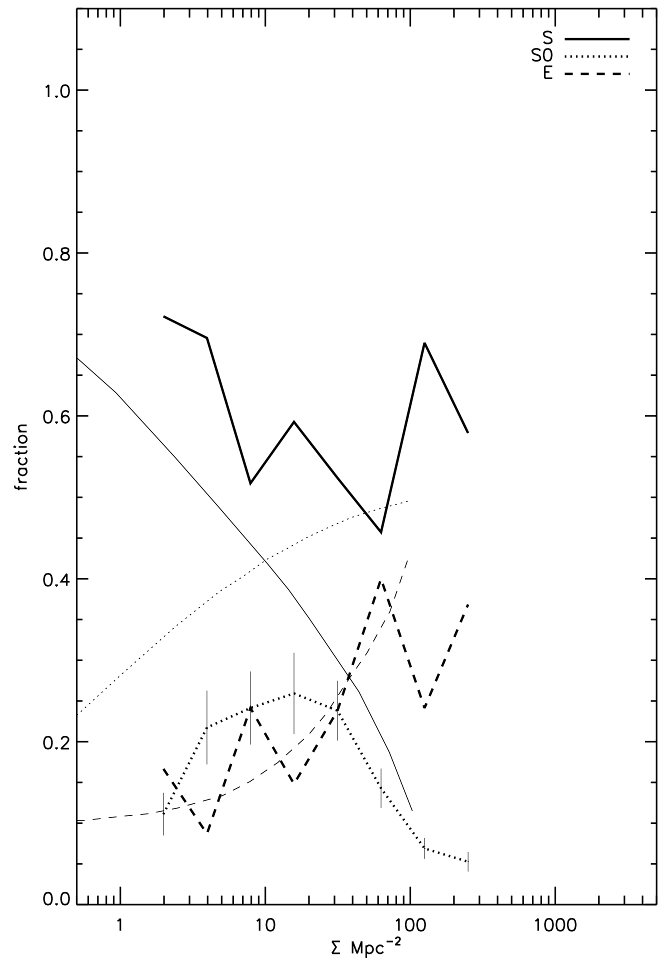

FIG. 5.—MDR for the cluster in the model C_1. We show the 1 σ error bars for the S0 fraction.

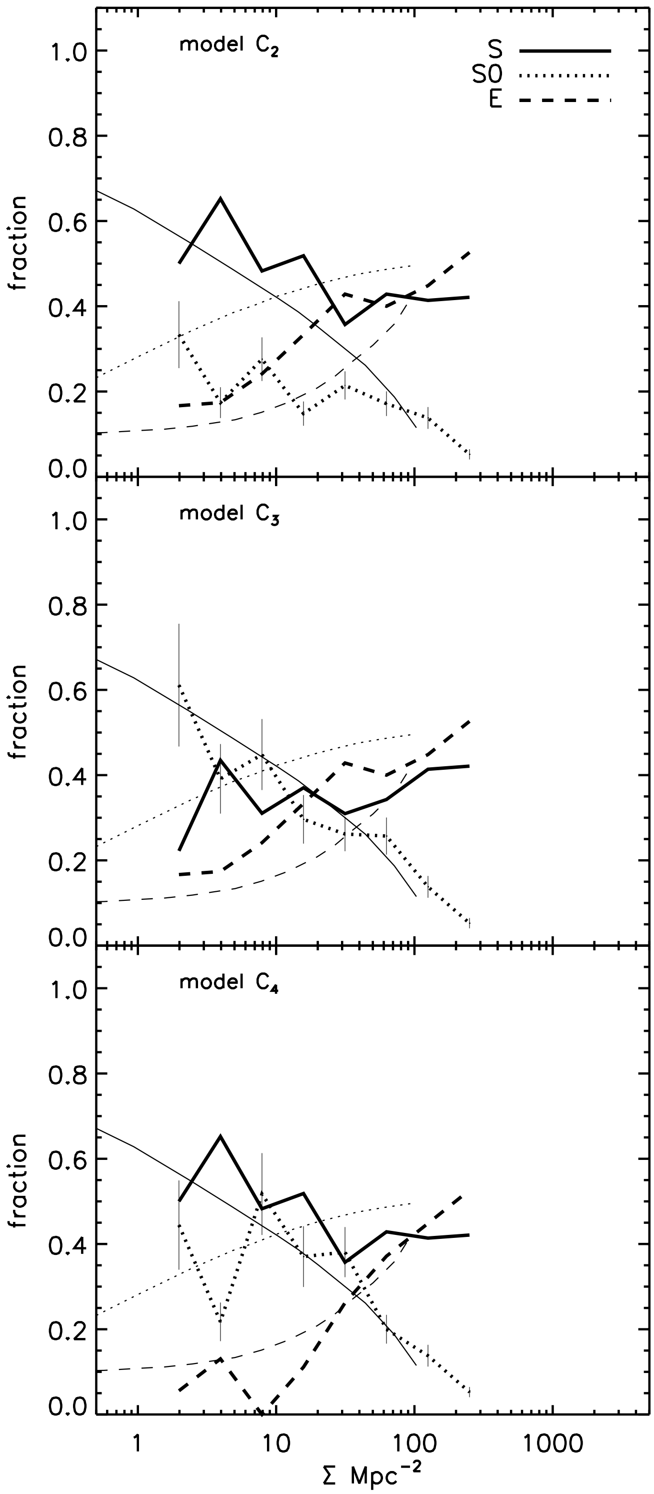

FIG. 6.—MDRs for the cluster in the model with $f_{\rm bulge} = 0.1$. The top, middle, and bottom panels show the MDRs in the model C_2, C_3, and C_4, respectively. We show the 1 σ error bars for the S0 fractions.

it hardly changes in the high-density regions. Above results mean that the galaxies in very high-density regions mainly separate into two types, i.e., bulge-dominated and disk-dominated galaxies, under the major merger hypothesis.

4. DISCUSSION

In this paper, we represent a new method that combines high-resolution N-body simulations with a semianalytic galaxy formation model for cluster galaxies. The high-resolution simulations enable us to identify and trace galactic halos within clusters directly. Therefore, we can obtain the three-dimensional distribution of the cluster galaxies and also we can incorporate the dynamical processes, for example merging and tidal stripping of the galactic halos in the clusters, into our modeling of galaxy formation. For the first study of the cluster galaxies using this method, we have shown the MDRs for the simulated clusters of galaxies with two cosmological models based on the merger-driven bulge formation scenario.

The model which reproduce the observed luminosity function well (model C) is successful in explaining the observed elliptical fraction as a function of the local density. However, any models cannot reproduce the observed trend in the distribution of the cluster S0s. In all models, the S0 fractions are too small, especially in the high-density regions.

We also examine the case in which the S0 galaxies in the cluster environment have the different B/D range from the S0 galaxies in the field, because Koopmann & Kenney (1998) found that the galaxies with low central concentration, which should be identified as spiral galaxies in the field, were often classified into the S0 type in clusters. We have confirmed that the S0 fraction are increased only in the low density regions even if we adopt lower threshold value of B/D between S and S0.

We then investigate how the parameter, $f_{\rm bulge}$, affects on the MDR. When we choose smaller $f_{\rm bulge}$, the early-type fraction is increased. In this case, however, the elliptical fraction is mainly increased, the shortage of S0s is then still significant. Even if we classify the high B/D spirals or the low B/D ellipticals as S0s in the model with small $f_{\rm bulge}$, this change increases the S0 fraction only in the low-density regions again. These results imply that, under the morphological evolution model only by the major mergers, the galaxies separate into two types, i.e., almost pure bulge and pure disk systems, in the high-density regions independent on the choice of the parameters and cosmologies.

The reason is probably considered as follows. In the model adopted here, a S0 galaxy is mainly formed by the disk formation after the last major merger. The efficiency of merging is, however, high before cluster formation, and then it rapidly decreases due to the large internal velocity dispersions of the clusters and the reduction of the size of tidally truncated halos as the mass of clusters grows. The accretion onto the galactic halos is also prevented by the strong tidal field after beginning of the cluster formation (Okamoto & Habe 1999). Hence, the cluster ellipticals formed by the mergers at high redshifts hardly change their morphologies into S0s by minor mergers or gas accretion, which form additional stellar disks.

As we mentioned in § 2.3, the morphological classification only by B/D is the simplest way and different from the Dressler's way. Essentially, S0s are not defined by their B/D but by the appearance of the galaxies (smooth disk, no strong spiral arms, etc.). Moreover, there is evidence that the MDR is more than just a B/D-density relation (e.g., Caon & Einasto 1995; Koopmann & Kenney 1998). In spite of above facts, we believe that our results about the deficiency of the S0 galaxies under the major merger hypothesis is robust, because there is a correlation between the Hubble type and B/D (Simien & de Vaucouleurs 1986) and our results are not changed by the choice of the parameters.

We conclude that the morphological evolution model by major mergers gives a good explanation for the distribution of the cluster ellipticals, while it cannot produce the S0 galaxies sufficiently. To reproduce the observed S0 fraction, other physical processes that directly change the morphology from spiral galaxies into S0 galaxies should be considered. For example, numerical simulations have shown that minor mergers produce galaxies resembling S0/Sa galaxies as merger remnants (Mihos & Hernquist 1994; Mihos et al. 1995; Walker et al. 1996). Although the bulge formation by the minor mergers are partly considered in our model and the model of Baugh et al. (1996), by incorporating some fraction of stars from accreting satellites into the bulge of a central galaxy, the starburst triggered by the minor mergers (Mihos & Hernquist 1994) and the processes which puffs up a stellar disk of the central galaxy by the minor mergers (Walker et al. 1996) are not involved. The ram-pressure stripping (Gunn & Gott 1972; Fujita & Nagashima 1999) and the galaxy harassment (Moore et al. 1996, 1998) are also promising processes to match the S0 fraction with the observed one. It is important to include such morphological evolution processes in the semianalytic modeling of galaxy formation, and it is left for further studies.

In the next paper, we will investigate whole properties of cluster galaxies in detail, i.e., colors, metalicities, velocities, and so on, using the method presented in this paper. We will also examine some morphological evolution processes other than major mergers.

We are grateful to A. Habe and Y. Fujita for useful discussions and valuable insights. We also thank the referee who led us to a substantial improvement of our paper. Numerical computation in this work was carried out on the HP Exemplar at the Yukawa Institute Computer Facility and on the SGI Origin 2000 at the Division of Physics, Graduate School of Science, Hokkaido University.

REFERENCES

Barnes, J. E. 1996, in ASP Conf. Ser. 92, Formation of the Galactic Halo—Inside and Out, ed. H. L. Morrison & A. Salajedini (San Francisco: ASP), 415

Baugh, C. M., Cole, S., & Frenk, C. S. 1996, MNRAS, 283, 1361

Benson, A. J., Cole, S., Frenk, C. S., Baugh, C. M., & Lacey, C. G. 2000, MNRAS, 311, 793

Binney, J., & Tremaine, S. 1987, Galactic Dynamics (Princeton: Princeton Univ. Press)

Bond, J. R., Cole, S., Efstathiou, G., & Kaiser, N. 1991, ApJ, 379, 440

Bower, R. G. 1991, MNRAS, 248, 332

Caon, N., & Einasto, M. 1995, MNRAS, 273, 913

Cole, S., Aragón-Salamanca, A., Frenk, C. S., Navarro, J. F., & Zepf, S. E. 1994, MNRAS, 271, 781

Couch, W. J., Ellis, R. S., Sharples, R. M., & Smail, I. 1994, ApJ, 430, 121

Dressler A. 1980, ApJ, 236, 351

Dressler A., et al. 1997, ApJ, 490, 577

Evrard, A. E., Summers, F. J., & Davis, M. 1994, ApJ, 422, 11

Fujita, Y., & Nagashima, M. 1999, ApJ, 516, 619

Gunn, J. E., & Gott, J. R. 1972, ApJ, 176, 1

Katz, N., Hernquist, L., & Weinberg, D. H. 1992, ApJ, 399, L109

Kauffmann, G. 1996, MNRAS, 281, 487

Kauffmann, G., & Charlot, S. 1998, MNRAS, 294, 705

Kauffmann, G., Colberg, J. M., Diaferio, A., & White, S. D. M. 1999, MNRAS, 397, 529

Kauffmann, G., White, S. D. M., & Guiderdoni, B. 1993, MNRAS, 264, 201

Kodama, T., & Arimoto, N. 1997, A&A, 320, 41

Koopmann, R. A., & Kenney, J. D. P. 1998, ApJ, 497, L75

Lacey, C., & Cole, S. 1993, MNRAS, 262, 627

Mihos, J. C., & Hernquist, L. 1994, ApJ, 425, L13

Mihos, J. C., Walker, I. R., Hernquist, L., Mendes de Olveira, C., & Bolte, M. 1995, ApJ, 447, L87

Moore, B., Katz, N., Lake, G., Dressler, A., & Oemler, A. 1996, Nature, 379, 613

Moore, B., Lake, G., & Katz, N. 1998, ApJ, 495, 139

Okamoto, T., & Habe, A. 1999, ApJ, 516, 591

———. 2000, PASJ, 52, 457

Press, W. H., & Schechter, P. L. 1974, ApJ, 187, 425

Roukema, B. F., Peterson, B. A., Quinn, P. J., & Rocca-Volmerrange, B. 1997, MNRAS, 292, 835

Salpeter, E. E. 1955, ApJ, 121, 161

Sandage, A., Binggeli, B., & Tammann, G. A. 1985, AJ, 90, 1759

Simien, F., & de Vaucouleurs, G. 1986, ApJ, 302, 564

Somerville, R. S., & Primack, J. R. 1999, MNRAS, 310, 1087

Summers, F. J., Davis, M., & Evrard, A. 1995, ApJ, 454, 1

Sutherland, R., & Dopita, M. A. 1993, ApJS, 88, 253

Toomre, A. 1977, in The Evolution of Galaxies and Stellar Populations, ed. B. M. Tinsley & R. B. Larson (New Haven: Yale Univ. Press), 401

Walker, I. R., Mihos, J. C., & Hernquist, L. 1996, ApJ, 460, 121